Effects of Poloxamer Inhomogeneities on Micellization in Water

Walther Batsberg,[†] Sokol Ndoni,[†] Christa Trandum,[‡] and Søren Hvidt*[,§]

Danish Polymer Centre, Risø National Laboratory, DK-4000 Roskilde, Denmark; MEMPHYS, University of Southern Denmark, DK-5230 Odense, Denmark; and Department of Chemistry, Roskilde University, DK-4000 Roskilde, Denmark

Received November 21, 2003

ABSTRACT: Pluronic P85 (poloxamer 235), which is a symmetrical PEO−PPO−PEO triblock copolymer of poly(ethylene oxide) and poly(propylene oxide), has been investigated by differential scanning calorimetry and chromatography. Interaction chromatography at critical conditions for PEO was used for chromatographic characterization and preparative separation of P85 according to PPO block lengths. The results show that the P85 sample is heterogeneous with respect to chemical composition and molar mass. P85 contains 12 wt % lower size impurities, which do not contribute to the main micellization transition. The shapes and widths of the micellization peaks observed in P85 thermograms are influenced by the distribution of PPO block lengths in P85, as shown from measurements on chromatographic fractions. PPO block lengths of the main P85 fraction follow a Poisson distribution closely. The characteristic temperatures of micellization, sphere-to-rod, and phase separation transitions observed in thermograms are influenced by polydispersity.

Introduction

Poloxamers have been studied extensively since they exhibit a fascinating range of structures in solution depending on concentration, copolymer composition, cosolutes, and temperature and since they are widely used as detergents in many applications.[1−3] Poloxamers are symmetrical triblock copolymers of poly(ethylene oxide)−poly(propylene oxide)−poly(ethylene oxide), with composition $EO_xPO_yEO_x$, where x and y denote the number of monomers per block. Early studies established that poloxamers are dissolved in water as individual polymer chains, unimers, at low temperatures and that micelles are formed with increasing temperatures[4−6] due to a difference in the interaction of water with PPO polymer blocks and PEO polymer blocks.[1−3] Both spherical and rodlike micelles have been observed experimentally.[7−11] Spherical micelles are formed with a core of PPO and a mantle of water-swollen PEO chains.[10,11] Micellization of poloxamers and other detergents is often analyzed in terms of a closed association model with a dynamic equilibrium between unimers and micelles

$$n \text{ unimers (aq)} \rightleftarrows \text{micelle}_n \text{ (aq)} \qquad (1)$$

where n is the number of unimers per micelle and denotes the cooperativity of the process. The value of n can be determined from the ratio of the van't Hoff enthalpy, ΔH_{vh}, and the calorimetric enthalpy, ΔH. Static light scattering studies on Pluronic P85 (poloxamer 235) from BASF show that micelles contain 30 unimers per micelle at 40 °C.[6] The value of n for poloxamers is determined both by the block length of PPO and by the ratio y/x, and n increases with temperature.[6,8] At low temperatures the equilibrium in eq 1 is shifted to the unimer side whereas micelles are strongly favored at high temperatures. The characteristic time scale for motions between unimers and micelles of poloxamers is faster than milliseconds,[12,13] which ensures that solutions are in near-equilibrium states.

A number of studies have shown that the simple association model in eq 1 is too simple to give an accurate description of the micellization process. Thermograms show a more gradual transition, which, however, can be accurately modeled if it is assumed that a smaller number of unimers aggregate prior to the formation of micelles.[14,15] For the large n values determined by light scattering the closed association model becomes nearly equivalent to a simple solubility model, corresponding to an infinite n, which predicts a sharp transition at the critical micellization temperature in differential scanning calorimetry (DSC) for large molar enthalpies of micellization. For the simple solubility model the equilibrium constant becomes 1/cmc, where cmc is the critical micellar concentration. The apparent van't Hoff enthalpy, ΔH_{vh}, can for this model be obtained from the temperature dependence of cmc

$$\ln \text{cmc} = \Delta H_{vh}/RT - \Delta S_{vh}/R \qquad (2)$$

where R is the gas constant, T is the absolute temperature, and ΔS_{vh} is apparent van't Hoff entropy.

It has been difficult to establish precise values of critical micellar concentrations for poloxamers since different techniques give different estimates.[1] One of the earliest observations[5] on poloxamers was an "anomalous micellization" which could be eliminated by filtration. Static and dynamic light scattering at low temperatures[6] showed the presence of large aggregates where only unimers should be present according to eq 1. The effects of these aggregates could be largely eliminated by extraction of copolymers in hexane.[16] Surface tension measurements,[9,17] size exclusion chromatography,[18] and force measurements[19] all show effects that have been attributed to heterogeneity of poloxamers. Poloxamers from different manufacturers with similar average compositions form micelles at very different temperatures.[20]

[†] Risø National Laboratory.
[‡] University of Southern Denmark.
[§] Roskilde University.
* Corresponding author: Tel +45-46-742477; FAX +45-46-743011; e-mail hvidt@ruc.dk.

10.1021/ma030567a CCC: $27.50
Published on Web 03/23/2004

In a recent study we have shown that the copolymers in micelles, formed at temperatures where both unimers and micelles are present, have higher relative PPO contents and molar masses than the remaining unimers.[21] These observations were in qualitative agreement with the predictions of Linse in his theoretical studies of the effects of heterogeneity and impurities on micellization.[22,23] Inhomogeneity of poloxamers is expected to broaden the transitions, as predicted theoretically by Linse.[23] These experimental observations and theoretical predictions suggest that inhomogeneities in especially the PPO block lengths have effects on micellization. Poloxamers are prepared by base-catalyzed polymerization,[1] and for these low molar mass polymers a molar mass distribution should be expected even in an ideal synthesis.

Micellization is mainly controlled by the PPO block length and concentration, whereas the PEO block lengths are of less importance.[24] Size exclusion chromatography can be used to purify poloxamers, but separation will occur depending on the combined sizes of PEO and PPO blocks. We have therefore used an interaction chromatographic method, originally developed by Pasch[25] for poloxamers with short PPO blocks ($y \leq 11$), which separates poloxamer block copolymers and PPO homopolymers according to PPO block lengths only. The chromatographic conditions have been optimized to give nearly critical conditions for the PEO blocks in such a way that fractionation only depends on PPO block lengths. We will refer to these conditions as CC−PEO. We have chosen to study Pluronic P85, which has a composition $EO_{27}PO_{39}EO_{27}$, according to the manufacturer, since this copolymer is one of the most studied poloxamers with convenient micellization and phase separation temperatures. The composition corresponds to a 51% weight fraction of EO and a molar mass of 4600 g/mol. We have characterized the Pluronic 80 series and P85 fractions resulting from interaction chromatography fractionation using NMR and DSC. P85 forms spherical and rodlike micelles in water and undergoes a phase separation at high temperatures.[6,7] These transitions for P85 and its fractions were investigated using differential scanning calorimetry (DSC) in order to investigate what factors determine the shape of transitions and the transition temperatures.

Materials and Methods

Polymer Samples. Pluronics L81, P84, P85, F87, and F88 were a gift from BASF (Parsippany, NJ). These copolymers of the Pluronic 80 series are expected to have the same PPO block ($y = 39$) but different PEO blocks. The expected x values are 6, 22, 27, 62, and 97 for L81, P84, P85, F87, and F88, respectively. The molar masses vary in the series from 2800 (L81) to 10 800 g/mol (F88). Homopolymers of PPO with average molar masses of 900 and 2000 g/mol were Pluriols from BASF. Homopolymers of PEO with average molar masses between 238 and 10 000 g/mol were from Merck. All copolymers and homopolymers investigated are expected to be diols. All aqueous solutions were made gravimetrically using double-distilled water. Concentrations are given as weight percent. Copolymers and homopolymers were dissolved in water under gentle shaking at 5 °C overnight.

Liquid Chromatography. Two types of liquid chromatography were used in this investigation. Size exclusion chromatography (SEC) was used to characterize copolymers according to hydrodynamic size. Interaction chromatography (IC) was used analytically and for preparative fractionation of P85 according to PPO block lengths. A Shimadzu HPLC system consisting of a LC-10AD pump, a CTO-10A column oven, and a RID 10A differential refractive index (RI) detector was used in both types of chromatography. The RI signal is proportional to the weight concentration, since PEO and PPO have very similar differential index increments.

The SEC column system consisted of a 50 mm × 7.5 mm PLgel Guard, a 300 mm × 7.5 mm PLgel Mixed-D, and a 250 mm × 10 mm Jordi-Gel DVB (100 Å). The columns and the RI detector were at room temperature (21.5 ± 0.5 °C), and THF was the eluent at a flow rate of 0.5 mL/min. Polymers were dissolved in THF to a concentration of 0.5%, and 200 μL was injected into the column system.

In interaction chromatography enthalpic interactions with the column packing material are used to separate a mixture of polymers. A search was made for chromatographic conditions where the elution was independent of the PEO block molar mass, whereas PPO blocks were eluted according to interaction chromatography. CC-PEO depend for a given column on eluent composition and temperature. The column for the analytical characterization was a 250 mm × 4.6 mm Nucleosil CN from Macherey-Nagel. The CC-PEO conditions were 44% methanol and 56% water by weight at a temperature of 50 °C at a flow rate of 0.5 mL/min. Polymers were dissolved in the eluent to a concentration of 0.2%, and 100 μL was injected into the column system. Preparative fractionations at CC-PEO were performed on the same column or on a 250 mm × 8 mm Nucleosil CN column at a flow rate of 2 mL/min.

NMR. The relative EO/PO compositions of Pluronic samples and P85 fractions were determined by NMR on samples dissolved in $CDCl_3$ with TMS as a reference. ^{1}H spectra were recorded on a Bruker 250 MHz instrument, and the PO/EO average block length ratios, y/x, were calculated from the integrals of peaks near 1.1 and 3.5 ppm, as described elsewhere.[21] The reproducibility of the relative EO content determinations was 0.3%.

Scanning Calorimetry. Differential scanning calorimetry was performed using a Nanocal scanning calorimeter from CSC (Calorimetry Science Corp., Provo, UT) with a cell volume of 0.322 mL. A few measurements were also made on a MC-2 scanning calorimeter from MicroCal (Northampton, MA) with a cell volume of 1.2396 mL at higher concentrations. Scans were performed on Pluronic solutions with concentrations between 0.01 and 10 wt % in water. Sample cells were loaded with a poloxamer preparation and the reference cells with water. Before each scan the sample was equilibrated for 50 min at the starting temperature (5 °C). Scans were performed with a scan rate of 20 °C/h between typically 5 and 85 or 95 °C. The thermal lag was negligible at this scan rate and lower scan rates. In general, only heating scans were employed for the study of the micellization process, but in a few cases cooling and reheating of solutions were also done. Data from both instruments were analyzed using ORIGIN software from MicroCal (Northampton, MA), as described elsewhere.[21] Micellization transition temperatures were reproducible to within 0.2 °C, and the enthalpies of micellization were reproducible within 3%.

Results

The members of the Pluronic 80 series are expected to have the same PPO block length, with 39 PO units corresponding to a PPO mass of 2260 g/mol. NMR analysis was used to determine the actual wt % EO in the samples. Results for the samples are summarized in Table 1 and are seen to be in reasonable agreement with the expected trend in the series. The last digit in the Pluronic nomenclature multiplied by 10 should roughly be the EO content in wt %. Micellization temperatures for Pluronic samples depend on copolymer concentration and composition and especially on the PPO block length. Solutions of Pluronic samples and solutions of PPO 2000 were made with a common PO concentration of 0.5 wt % and measured in the DSC instrument between 5 and 95 °C. From the scan rate

Table 1. Characterization and DSC Results of Pluronic Samples; EO Content from NMR, Low Size Contaminant from SEC, and Micellization Peak Transition and Half-Width Temperatures from DSC of Solutions with a PPO Concentration of 0.5 wt %

sample	EO content (wt %)	contaminant (wt %)	T_m (°C)	ΔH_m (J/g PO)	$T_{1/2}$ (°C)
L81	22.3	7.5	29.6	110.5	10.3
P84	45.9	7.5	34.4	106.5	9.1
P85	51.3	12.2[a]	34.1	97.2	9.0
F87	71.7	10.3	38.9	94.8	9.5
F88	80.8	13.7	39.4	82.6	9.7
PPO 2000			22.1	129.2	5.5

[a] Standard deviation of ±0.5% from 10 different chromatograms.

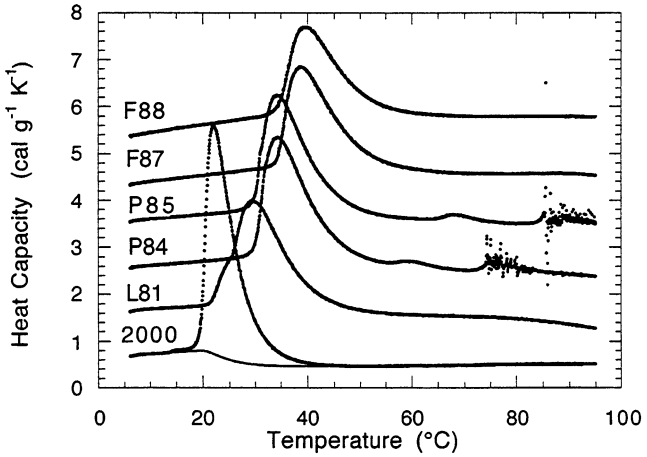

Figure 1. Thermograms of aqueous solutions of PPO 2000 and the Pluronic 80 series. The heat capacities per gram of poly(propylene oxide) are plotted against temperature. Curves are shifted vertically for clarity. Poloxamer concentrations vary such that poly(propylene oxide) concentrations for all solutions are 0.5 wt %. A progress baseline is shown for the PPO 2000 solution.

and the difference in heat flow between the sample cell and the reference cell, which was filled with water, the heat capacity at constant pressure, C_p, was obtained. The thermograms in Figure 1 show the heat capacities plotted against temperature for all solutions. The thermograms are expected to be near-equilibrium curves, since the cooling and repeated heating scans gave identical curves for several samples. The thermograms are dominated by a large broad endothermic transition for all samples. The main transitions for P84 to F88 are assigned to a gradual formation of spherical micelles.[26] The transition for PPO 2000 is due to phase separation, and the L81 transition occurs at temperatures where solutions become turbid, suggesting either phase separation or formation of larger structures such as sheets. Two minor endothermic transitions can be seen for P84 and P85 above the micellization transition. These transitions have been assigned to the sphere-to-rod transition and phase separation, respectively, at increasing temperatures.[6,8]

Figure 1 shows that micellization is characterized by a negative ΔC_p for all 80 series samples, and progress baselines were constructed connecting linear baselines before and after the transitions.[21] The enthalpy of micellization, ΔH_m, can be obtained by integration of the excess capacities over the baseline. Values of ΔH_m in J/(g PO) are summarized in Table 1 together with the peak transition temperatures, T_m, corresponding to the temperature at maximum heat capacity. The figure also shows that the peak for PPO 2000 is sharper than

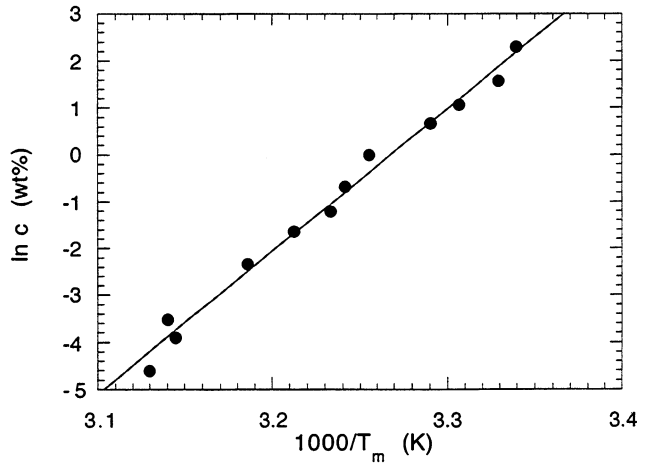

Figure 2. Concentration dependence of the micellar peak transition temperature is plotted in the form of a van't Hoff plot of P85 DSC data. From the slope of the linear least-squares fit a van't Hoff enthalpy of 250 kJ/mol is obtained.

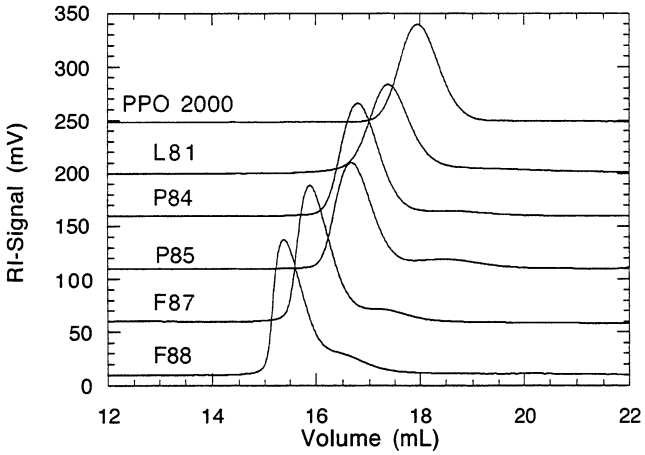

Figure 3. Size exclusion chromatography of PPO 2000 and the Pluronic 80 series. The exclusion and total volumes of the column are 12 and 25 mL, respectively.

the peaks for the 80 series. The half-width, $T_{1/2}$, of the transition was used as a measure of the width. Values of $T_{1/2}$ are summarized in Table 1.

P85 micellization was studied using both calorimeters at concentrations between 0.01 and 10 wt %. The micellization peak temperature decreases with increasing concentration. The results are shown in Figure 2 in the form of a van't Hoff plot, where the natural logarithm of concentration is plotted against $1/T_m$. The thermograms show that the onset temperature for micellization, T_{on}, is lower than T_m, as illustrated in Figure 1. According to the simple solubility model, they should be equal. The use of the simple solubility model in eq 2 is therefore questionable, but it is seen in Figure 2 that the data follow a linear relation quite well. From the slope an apparent van't Hoff enthalpy of 250 kJ/mol is obtained.

The widths of the transitions in Figure 1 suggest either low cooperativity during micellization (small n values) or polydispersity effects. To investigate the latter possibility, all samples were analyzed by size exclusion chromatography, as shown in Figure 3. As expected, copolymers elute in the order of decreasing molecular mass from F88 to L81 followed by PPO 2000. The figure, however, also shows that all the copolymers contain varying amounts of smaller size contaminants, which

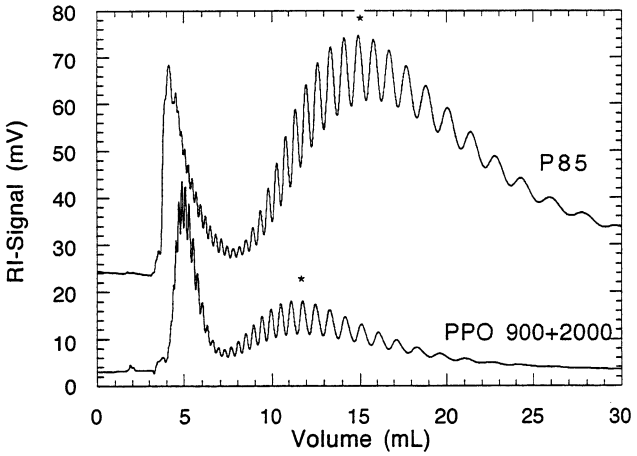

Figure 4. Critical interaction chromatography of P85 at 50 °C with a 44 wt % methanol in water eluent with a refractive index detector. Chromatogram of a mixture of PPO 900 and 2000 under the same elution conditions is also shown. The peaks marked with * correspond to PO_{31} and PO_{36} for the PPO mixture and P85, respectively. The total volume of the column is 3 mL.

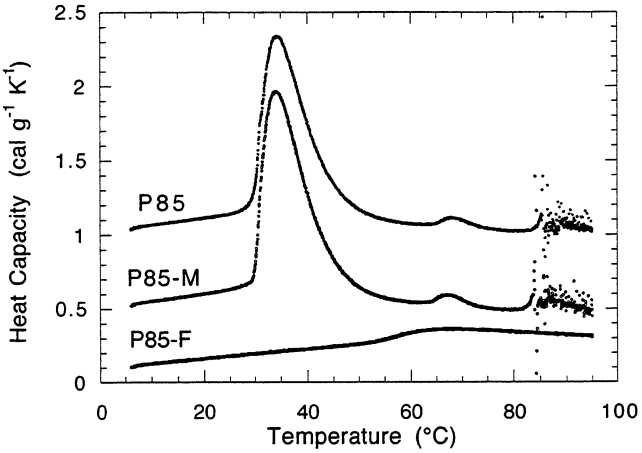

Figure 5. Thermograms of unfractionated P85 and of the front (P85-F) and main (P85-M) fractions obtained after separation on a CN column. The heat capacities per gram of polymer are plotted against temperature. Concentrations for all solutions are 1.0 wt %.

elute as a peak or shoulder following the main peak. Estimates of the relative content of lower size component was obtained from the fractional area of the peaks of the RI signal. The analysis based on 10 different P85 chromatograms shows that this sample contain 12.2% lower size material. Values for all copolymers are summarized in Table 1.

To investigate the influence of polydispersity on micellization thermograms, P85 was separated by an interaction chromatographic method. Since micellization is primarily determined by the PPO block length, separation should reflect this length rather than the total copolymer length. In critical interaction chromatography of a block copolymer the elution volume is independent of one of the block lengths. A CN column with MeOH/water as mobile phase was chosen as this allows separation of PPO over a wide range of y under isocratic elution conditions at constant temperature. The critical concentration of MeOH and temperature conditions were found where PEOs with molecular masses between 238 and 10 000 g/mol all eluted close to the total volume of the column. Such conditions occurred at 44 wt % MeOH at 50 °C. Under these critical conditions, CC-PEO, elution is determined only by the PPO block lengths. Elution of a mixture of PPOs 900 and 2000 under CC-PEO shows a finger pattern of peaks, where each peak corresponds to one specific PPO block length, as illustrated in Figure 4. Several of the peaks were collected and analyzed by mass spectrometry which enabled the assignment of the degree of polymerization for each peak. The maximum of the PPO 900 peaks corresponds to a PO_{14}, and from this and other similar identifications the rest of the peaks in both PPO 900 and PPO 2000 can be assigned. The areas under the peaks are proportional to the weight concentration of the copolymers since the differential refractive index increments of PPO and PEO are similar. The highest peak signal for PPO 2000 in Figure 4 corresponds to a PO_{32}, but the peak with the largest area is PO_{34}, which corresponds to a molecular mass of 1990 g/mol. When P85 is eluted under the same critical conditions a finger pattern is also observed as shown in Figure 4. The dominating peaks of P85 elute after the main PPO 2000 peaks, with a maximum height peak corresponding to PO_{36} and a maximum area at PO_{38}. The figure also shows that P85 contains components, which elute earlier and contain PPO block lengths similar to PPO 900 as seen from the finger pattern, as well as another impurity, which is not resolved under the chromatographic conditions used here. The fractional area of the early eluting group of peaks corresponds to 12% of the total area. The figure therefore illustrates that P85 is inhomogeneous in two respects: P85 contains a distribution of PPO block lengths around PO_{38}, and in addition, 12% of the P85 sample has a much smaller PPO block length.

To investigate whether the smaller size contaminants have any effect on the micellization, a preparative separation was performed using the same column and CC-PEO. The first group of peaks containing the contaminants was collected, and after that repeated injections of 100% MeOH were made in order to elute the main P85 components, which were also collected. The front fraction, called P85-F, and the main component fraction, P85-M, were then vacuum-dried. After 12 collections 11 mg of P85-F and 83 mg of P85-M were obtained. This corresponds to a relative P85-F content of 11.7%. The fractions were redissolved in water to give 1.0 wt % solutions, and the concentrations were further checked by SEC chromatography using unpurified P85 as a reference. The thermograms obtained for the two fractions are shown in Figure 5. The figure shows very similar shaped thermograms for P85 and P85-M, but no peak for P85-F at temperatures where micelles are formed for P85. P85-F shows only a very broad peak above 60 °C with a low area. Thermograms were analyzed as described above, and the results for P85 and the two fractions are shown in Table 2. It is seen that the transition temperatures are slightly lower for P85-M than for P-85, but more importantly ΔH_m is significantly higher (13%) for P85-M. This suggests that the 12% smaller components in P85, which were removed by the chromatographic method, do not contribute to the micellization part of the thermogram and perhaps do not even become a part of the micelles.

The other type of polydispersity in P85 is due to the distribution of PPO block lengths around a mean value. CN critical chromatography at CC-PEO was used again to check whether this distribution has any effect on the P85 thermograms. The main group of P85 peaks was

Table 2. Characterization of P85 Fractions by NMR and DSC; Onset, Peak, and Half-Width Temperatures of Micellization; T_{SR} and T_{FS} Are Peak Sphere-to-Rod and Onset Phase Separation Temperatures, Respectively[a]

sample	EO content (wt %)	T_{on} (°C)	T_m (°C)	ΔH_m (J/g)	$T_{1/2}$ (°C)	T_{SR} (°C)	T_{FS} (°C)
P85	51.3	29.2	34.3	49.0	9.2	67.8	83.5
P85-M	48.0	29.2	34.1	55.5	8.9	67.5	82.7
P85-F	77.2	52.6	66.5	6.6	20.9		
Fr1	51.0	37.1	40.0	53.3	5.7	71.9	>85
Fr2	49.5	31.9	34.7	58.6	4.9	60.4	75.7
Fr3	42.1	27.5	30.3	64.6	4.5	49.5	62.7

[a]All concentrations for DSC are 1 wt % in water.

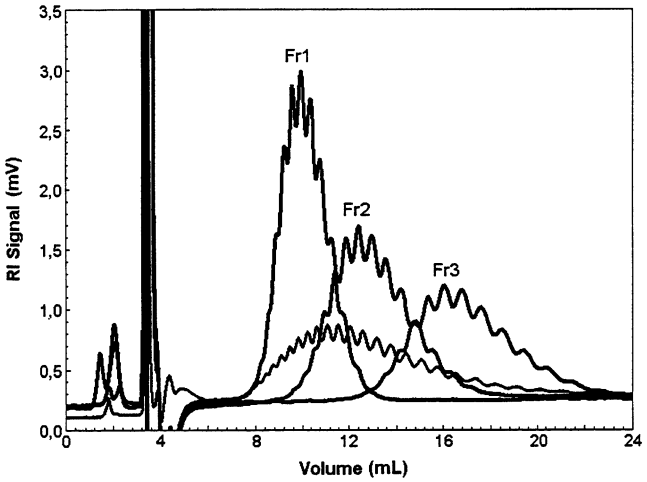

Figure 6. Elution profiles under critical conditions of P85 and of three P85 fractions obtained by preparative interaction chromatography at critical conditions.

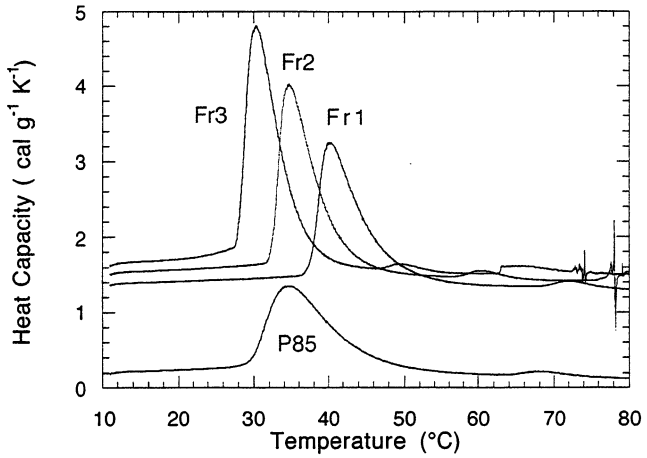

Figure 7. Thermograms of unfractionated P85 and of the three fractions shown in Figure 6. The heat capacities per gram of polymer are plotted against temperature. All concentrations are 1 wt %.

separated into three fractions: before, around, and after the main P85 peak. These fractions, labeled Fr1−Fr3, were then vacuum-dried and dissolved in water. Chromatograms of the three fractions at critical conditions are shown in Figure 6. It is seen that Fr1 only contains shorter PPO blocks and that Fr3 only contains longer PPO blocks than the dominating peak in P85. Fr2 contains average and slightly longer PPO blocks than the average blocks in P85. The relative EO content of the fractions from NMR is shown in Table 2. Thermograms of the three fractions and of P85 at a concentration of 1.0 wt % are shown in Figure 7. The longer PPO chains in Fr3 result in a lower T_m, and a difference in micellization transition temperatures of Fr3 and Fr1 of

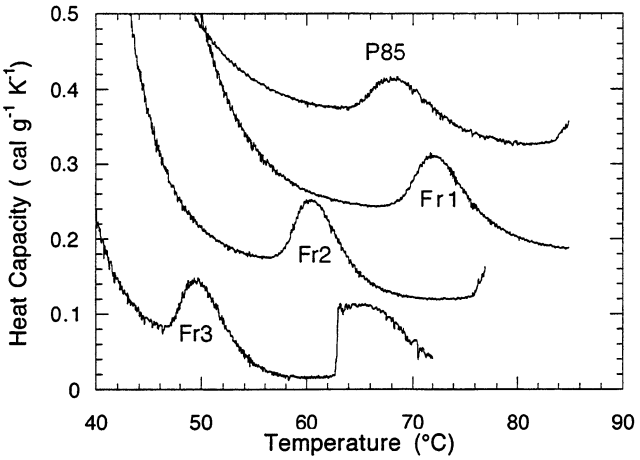

Figure 8. High-temperature part of the thermograms in Figure 7. The sphere-to-rod and phase separation transitions are shown for P85 and the three P85 fractions. High-temperature data points for Fr2 and Fr3 are not shown for clarity.

10 °C is seen. The figure also shows the thermogram of P85 at the same concentration. By comparison with the fractions, it is seen that the wider P85 transition covers nearly the same temperature range as the three fractions combined. Thermodynamic data for the fractions and for P85 are summarized in Table 2. An expanded view of the high-temperature part of the thermograms is shown in Figure 8. The sphere-to-rod transition for P85 results in a peak around 68 °C, and the start of the phase separation is at 84 °C (see also Figure 1). The PPO distribution has a dramatic effect on both transitions as seen for the three fractions. Fr1 has higher transition temperatures than P85 and phase separation does not occur below 85 °C, whereas Fr2 and Fr3 have lower transition temperatures. It should also be noted that the P85 transitions are not simply a sum of contributions from the three fractions as seen for the micellization peak.

CC-PEO was also used to analyze the other members of the Pluronic 80 series on two CN columns in series. Finger patterns were seen for all the samples, as illustrated for P84, F87, and F88 in Figure 9. All the samples show a distribution of PPO block lengths. The peak maximum signals correspond to PO_{37}, PO_{38}, and PO_{42} for P84, F87, and F88, respectively, as counted from the PPO 2000 maximum which corresponds to PO_{32}. These values are close to the peak value at PO_{36} found for P85 from the distribution in Figure 4. The figure shows that all three samples contain contaminants, which elute between the total volume of the column and the main group of peaks assigned to triblock copolymers.

Discussion

The results obtained in this study have shown that P85 contains 12% by mass lower size contaminants.

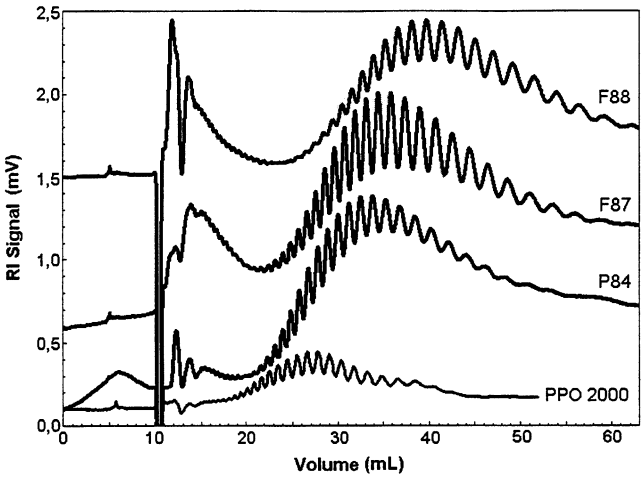

Figure 9. Critical interaction chromatography of P84, F87, F88, and PPO 2000. The total volume of the column is 10 mL. Polymers were dissolved in eluent with a few percent excess water.

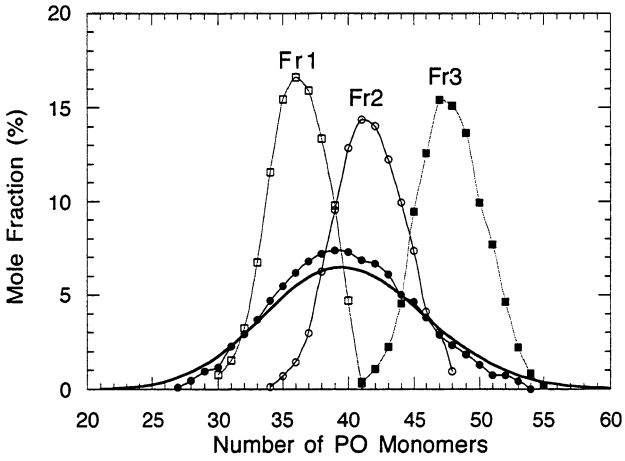

Figure 10. PPO block length distributions of P85 (filled circles) and of fractions Fr1 to Fr3. A Poisson distribution for an average polymerization step length of 38 is shown as the smooth curve.

Similar estimates of the content are obtained by both SEC in Figure 3, by interaction chromatography in Figure 4, and by the masses of P85-F and P85-M. The other members of the 80 series also contain varying amounts of lower size contaminates, as seen in Figures 3 and 9. Several other Pluronic samples have been investigated by SEC (data not shown), and especially higher molecular mass samples and samples with large PPO blocks show a high percentage of low molar mass impurities. About 18% low size impurities have been detected in Pluronic F127.[27] The presence of these contaminants is important for thermodynamic studies by e.g. DSC. Our DSC results suggest that these contaminants do not contribute to the micellization transition of the rest of the sample. This interpretation is consistent with SEC results for Pluronic F127 at elevated temperatures[18] and centrifugation experiments of P94.[21] The calculated values of ΔH and ΔS per mole of poloxamer copolymer will be underestimated if concentrations are not corrected for the presence of impurities, as demonstrated for P85 and P85-M in Table 2.

Poloxamers are prepared by anionic polymerization, and for this type of synthesis a distribution of polymer length should be anticipated. Besides the lower size contaminants P85 also consists of copolymers with a distribution of PPO block lengths as shown in Figure 4. The three fractions Fr1 to Fr3 in Figure 6 have on the average 33, 39, and 45 PO units per PPO block. These values correspond to PPO masses of 1914, 2262, and 2610 g/mol. From the NMR composition in Table 2 the total mass of the two PEO blocks is 1992, 2036, and 1898, corresponding to PEO block lengths of 23, 23, and 22, respectively. The three fractions have therefore almost identical average PEO block lengths with 23 EO units. This shows that the average length of the PEO blocks is unaffected by the PPO block lengths, but there is undoubtedly also a statistical distribution of PEO block lengths. The total average composition of Fr1 is therefore $EO_{23}PO_{33}EO_{23}$. Fr2 and Fr3 are similarly $EO_{23}PO_{39}EO_{23}$ and $EO_{22}PO_{45}EO_{22}$, respectively. These compositions show that the fractions obtained from the original poloxamer 235 should be labeled as poloxamers 195, 235, and 264 or as Pluronics P75, P85, and P94.

Figure 4 shows that PPO block lengths between at least 27 and 54 are observed in the sample. This gives the impression of a wide PPO distribution. Since each PPO block is thought, on the average, to have the same PEO blocks with 23 EO units, corresponding to a total mass of 2042 g/mol, the chromatogram in Figure 4 can be used to calculate the relative content of each PPO block in the sample. The areas under the peak are proportional to the mass of the component. For a peak with y PO units the molar mass in g/mol is $(58y + 2042)$. With the mass and molar mass the relative number distribution of the PO units can be calculated as shown in Figure 10. Similar calculations were also performed for Fr1, Fr2, and Fr3. Ideally the P85 distribution should follow a Poisson distribution, and this prediction is shown on the same figure for an average polymerization of 38 steps. The agreement with the experimental data for P85 is seen to be quite good. With the distributions the heterogeneity index for the PO blocks M_w/M_n can be obtained. The calculated values from the chromatograms are 1.0186 for P85 and 1.0044 (Fr1), 1.0044 (Fr2), and 1.0029 (Fr3). The Poisson distribution, for a number-average degree of polymerization of 38, predicts a value of 1.025. The results show that the PPO blocks in P85 without the impurities have an even narrower distribution than the Poisson distribution and that the fractions have extremely narrow distributions.

It has been recognized earlier that the widths of poloxamer thermograms are not consistent with a closed association mechanism with n values corresponding to the number of unimers per micelle.[14,15,21] For typical n values of 20−60 the leading edge of the thermogram is predicted to be very sharp, and the onset and maximum temperatures in the thermograms should almost be identical. Poloxamers, however, show a much more slowly rising leading edge, which has been taken as evidence for a multistep mechanism, where a few unimers first aggregate followed by an athermal formation of micelles.[15] This model has been most successful in fitting experimental thermograms for many poloxamers. The results presented here in Figure 8 and in Table 2, however, show that the rising edge in P85 is much reduced for the P85 fractions and that the widths of the transitions for the fractions are also much smaller than for unpurified P85. Our results therefore suggest that the broad micellization transition is due to a gradual process in which copolymers with shorter PPO blocks are gradually incorporated into micelles with increasing temperature. This interpretation is consis-

tent with the observation[21] that the relative PPO content in micelles exceeds the PPO content of the unimers during micellization.

Fraction 2 has a composition close to the average composition of the unfractionated P85. For this fraction the molar enthalpy of micellization can be calculated from its average mass of 4298 g/mol and its specific micellization enthalpy of 58.6 J/g. Fraction 2's molar enthalpy of 252 kJ/mol is in excellent agreement with the van't Hoff enthalpy value of 250 kJ/mol for P85, determined from the concentration dependence of the peak transition temperatures in Figure 2. This shows that a simple solubility model or an association model with a large n describe the properties quite well. The T_m values for P85 and Fr2 are also more similar than their T_{on} values, and this suggests that T_m is a more characteristic critical micellization temperature for polydisperse copolymers than T_{on}, since the latter is more influenced by the polydispersity.

The calorimetric enthalpies for the 80 series with similar PPO blocks vary significantly with PEO block lengths. The enthalpies per gram of PO are all smaller than the value for PPO 2000, even if the ΔH_m values are corrected for the content of impurities. The reason for this is unclear at present but may indicate that the smaller PPO cores of micelles with large PEO blocks are not fully dehydrated or have a larger relative surface of PPO core in contact with water. The results also demonstrate that the transition temperatures are dependent on the PEO block length. T_m values for all members of the 80 series exceed the transition temperature of PPO 2000, which even has a smaller PPO block. The sphere-to-rod transition and phase separation depend on the relative EO/PO volume ratio. A large value favors spherical values. When temperature is increased, water becomes a poorer solvent for PEO and the volume ratio decreases, which results in the formation of rodlike micelles. This is illustrated in Figure 1 where it is seen that P84, with shorter PEO chains than in P85, forms rodlike micelles at a lower temperature. The fractions in Figure 8 demonstrate this nicely, and it is seen that Fr3 (P94) forms rodlike micelles at a temperature even below the temperature observed for P84, which has shorter PEO blocks than P85. The phase separation temperature is also dependent on the relative EO/PO content and varies considerably between the fractions. The transition temperatures for the three purified fractions are either lower or higher than the temperatures observed for the unfractionated P85. The fact that fairly sharp transitions are seen for P85 shows that the structures formed at high temperatures are mixed micelles which can accommodate copolymers with both short and long PPO blocks.

Conclusions

Our results have demonstrated that all the members of the Pluronic 80 series contain lower size impurities. For P85 different techniques show 12% impurities by mass. The micellization enthalpy of P85 increases after removal of these impurities. Critical interaction chromatography enables a detailed investigation of the PPO distribution in poloxamers. Even though the distribution of PPO blocks is as narrow as the Poisson distribution, fractionation of P85 results in sharper micellization transitions. The sphere-to-rod and phase separation temperatures are also very dependent on the PPO distribution. Shapes of micellization curves, micellization enthalpies, and transition temperatures are dependent on the heterogeneity of P85.

The results obtained here are believed to be of importance for many other types of amphiphilic block copolymers. Molar mass distributions of copolymers should be expected, and micellization should therefore be a gradual process. Different techniques, e.g., light scattering, dye solubility, surface tension, and DSC, are sensitive to different properties during micellization and may therefore give different estimates of e.g. cmc due to heterogeneity. In addition, contaminants in the copolymer samples, such as the low molecular size impurities in P85 detected in this study, may reduce the values of the micellization enthalpy compared to that of a purified sample.

Acknowledgment. We thank Lars Duelund for help with the DSC experiment and Lotte Nielsen for assistance with many of the HPLC experiments.

References and Notes

(1) Alexandridis, P.; Hatton, T. A. *Colloids Surf. A* **1995**, *96*, 1−46.
(2) Almgren, M.; Brown, W.; Hvidt, S. *Colloid Polym. Sci.* **1995**, *273*, 2−15.
(3) Alexandridis, P.; Lindman, B. *Amphiphilic Block Copolymers: Self-Assembly and Applications*; Elsevier: Amsterdam, 2000.
(4) Rassing, J.; Attwood, D. *Int. J. Pharm.* **1983**, *13*, 47−55.
(5) Zhou, Z.; Chu, B. *Macromolecules* **1988**, *21*, 2548−2554.
(6) Brown, W.; Schillén, K.; Almgren, M.; Hvidt, S.; Bahadur, P. *J. Phys. Chem.* **1991**, *95*, 1850−1858.
(7) Schillén, K.; Brown, W.; Johnsen, R. M. *Macromolecules* **1994**, *27*, 4825−4832.
(8) Mortensen, K.; Brown, W. *Macromolecules* **1993**, *26*, 4128−4135.
(9) Wanka, G.; Hoffmann, H.; Ulbricht, W. *Macromolecules* **1994**, *27*, 4145−4159.
(10) Glatter, O.; Scherf, G.; Schillén, K.; Brown, W. *Macromolecules* **1994**, *27*, 6046−6054.
(11) Mortensen, K.; Pedersen, J. S. *Macromolecules* **1993**, *26*, 805−812.
(12) Fleischer, G. *J. Phys. Chem.* **1993**, *97*, 517−521.
(13) Hvidt, S. *Colloids Surf. A* **1996**, *112*, 201−207.
(14) Armstrong, J.; Chowdhry, B.; O'Brien, R.; Beezer, A.; Mitchell, J.; Leharne, S. *J. Phys. Chem.* **1995**, *99*, 4590−4598.
(15) Paterson, I.; Armstrong, J.; Chowdhry, B.; Leharne, S. *Langmuir* **1997**, *13*, 2219−2226.
(16) Hvidt, S.; Jørgensen, E. B.; Schillén, K.; Brown, W. *J. Phys. Chem.* **1994**, *98*, 12320−12328.
(17) Wanka, G.; Hoffmann, H.; Ulbricht, W. *Colloid Polym. Sci.* **1990**, *268*, 101−117.
(18) Malmsten, M.; Lindman, B. *Macromolecules* **1992**, *25*, 5440−5445.
(19) Schillén, K.; Claesson, P. M.; Malmsten, M.; Linse, P.; Booth, C. *J. Phys. Chem. B* **1997**, *101*, 4238−4252.
(20) Yu, G. E.; Altinok, H.; Nixon, S. K.; Booth, C.; Alexandridis, P.; Hatton, T. A. *Eur. Polym. J.* **1997**, *33*, 673−677.
(21) Hvidt, S.; Trandum, C.; Batsberg, W. *J. Colloid Interface Sci.* **2002**, *250*, 243−250.
(22) Linse, P. *Macromolecules* **1994**, *27*, 2685−2693.
(23) Linse, P. *Macromolecules* **1994**, *27*, 6404−6417.
(24) Alexandridis, P.; Holzwarth, J. F.; Hatton, T. A. *Macromolecules* **1994,** *27*, 2414−2425.
(25) Gorshkov, A. V.; Much, H.; Becker, H.; Pasch, H.; Evreinov, V. V. *J. Chromatogr.* **1990**, *523*, 91−102.
(26) Brown, W.; Schillén, K.; Hvidt, S. *J. Phys. Chem.* **1992**, *96*, 6038−6044.
(27) Yu, G.-E.; Deng, Y.; Dalton, S.; Wang, Q.-C.; Attwood, D.; Price, C.; Booth, C. *J. Chem. Soc., Faraday Trans.* **1992**, *88*, 2537−2544.

MA030567A